Inorganic Chemistry
Article

Inorg. Chem. **2011**, *50*, 2015–2027 **2015**
DOI: 10.1021/ic101624y

Syntheses, and Optical, Fluorescence, and Nonlinear Optical Characterization of Phosphine-Substituted Terthiophenes

Qun Zhao,[†] Jianwei Wang,[‡] Jason L. Freeman,[†] Makeba Murphy-Jolly,[†] Ashley M. Wright,[§] Debra J. Scardino,[§] Nathan I. Hammer,[§] Christopher M. Lawson,[‡] and Gary M. Gray*,[†]

[†]*Department of Chemistry, and* [‡]*Department of Physics, The University of Alabama at Birmingham, 1530 Third Avenue S., Birmingham, Alabama 35294, United States, and* [§]*Department of Chemistry and Biochemistry, Coulter Hall 113, The University of Mississippi, Oxford, Mississippi 38677, United States*

Received August 10, 2010

Earlier studies of phosphine-substituted terthiophenes have demonstrated that some of these materials exhibit nonlinear absorption at 532 nm. However, this wavelength is significantly removed from the linear absorption maxima of the complexes, suggesting that better nonlinear absorption might be observed at wavelengths closer to the linear absorption maxima. To investigate this possibility, a library of compounds has been prepared either by varying the group attached to the nonbonding pair of electrons on the phosphorus atoms of 5,5″-bis(diphenylphosphino)-2,2′:5′,2″-terthiophene (PT_3P), or by introducing additional substituents on the 5″-position of 5-(diphenylphosphino)-2,2′:5′,2″-terthiophene (PT_3). All these compounds have been characterized using multinuclear NMR, UV–vis, and fluorescence spectroscopy. The compounds are strongly fluorescent, and both the fluorescence wavelength and the intensity depend upon the thiophene substituents. The nonlinear optical properties have also been evaluated at various wavelengths in the blue region. Each compound exhibits reverse saturable absorption, and the intensity of the reverse saturable absorption at a particular wavelength depends on the chemical structure of the compound.

Introduction

Materials exhibiting third-order nonlinear optical properties have been investigated for important applications such as optical switching,[1,2] optical power limiting,[3,4] and optical computing.[5] A large number of conjugated metal–organic macrocycles, including various metalloporphyrins[6–9] and metallophthalocyanines,[10–15] display reverse saturable absorption in the green region of the visible spectrum. Numerous materials are also known to exhibit two-photon absorption in the red and near-infrared regions.[16–22] However, only one material showing nonlinear absorption (NLA) in the blue region of the visible spectrum has been reported.[23]

---

*To whom correspondence should be addressed. Phone: (205) 934-8294. Fax: (205) 934-2543. E-mail: gmgray@uab.edu.

(1) Sun, S. Dalton, L. R. *Introduction to Organic Electronic and Optoelectronic Materials and Devices*; CRC Press, Taylor & Francis Group: Boca Raton, FL, 2008.

(2) Interrante, L. V.; Hampden-Smith, M. J. *Chemistry of Advanced Materials: An Overview*; Wiley-VCH: New York, 1998.

(3) Spangler, C. W. *J. Mater. Chem.* **1999**, *9*, 2013–2020.

(4) Tuff, L. W.; Boggess, T. F. *Prog. Quantum Electron.* **1993**, *17*, 299–338.

(5) Dolev,S.; Haist, T.; Oltean, M. In *Proceedings of the First International Workshop on Optical SuperComputing*, Vienna, Austria, August 26, 2008; Springer: New York, 2008.

(6) Sun, W.; Byeon, C. C.; McKerns, M. M.; Lawson, C. M.; Gray, G. M.; Wang, D. *Appl. Phys. Lett.* **1998**, *73*, 1167–1169.

(7) Sun, W.; Byeon, C. C.; Lawson, C. M.; Gray, G. M.; Wang, D. *Appl. Phys. Lett.* **1999**, *74*, 3254–3256.

(8) Sun, W.; Byeon, C. C.; Lawson, C. M.; Gray, G. M.; Wang, D. *Appl. Phys. Lett.* **2000**, *77*, 1759–1761.

(9) Byeon, C. C.; McKerns, M. M.; Sun, W.; Nordlund, T. M.; Lawson, C. M.; Gray, G. M. *Appl. Phys. Lett.* **2004**, *84*, 5174–5176.

(10) Hanack, M.; Schneider, T.; Barthe, M.; Shirk, J. S.; Flom, S. R.; Pong, G. S. *Coord. Chem. Rev.* **2001**, 235–258.

(11) de la Torre, G.; Vazquez, P.; Agullo-Lopez, F.; Torres, T. *Chem. Rev.* **2004**, *104*, 3723–3750.

(12) Chen, Y.; Hanack, M.; Blau, W. J.; Dini, D.; Liu, Y.; Lin, Y.; Bai, J. *J. Mater. Sci.* **2006**, *41*, 2169–2185.

(13) Sathiyamoorthy, K.; Vijayan, C.; Varma, S. *Langmuir* **2008**, *24*, 7485–7491.

(14) Chen, Z.; Zhong, C.; Zhang, Z.; Li, Z.; Niu, L.; Bin, Y.; Zhang, F. *J. Phys. Chem. B* **2008**, *112*, 7387–7394.

(15) Venkatram, N.; Narayana Rao, D.; Giribabu, L.; Venugopal Rao, S. *Appl. Phys. B: Laser Opt.* **2008**, *91*, 149–156.

(16) Perry, J. W.; Hales, J. M.; Chi, S.; Cho, J.; Odom, S.; Zhang, Q.; Zheng, S.; Schrock, R.; Screen, T. E. O.; Anderson, H. L.; et al. *Polym. Prepr.* **2008**, *49*, 989–990.

(17) Hales, J. M.; Zheng, S.; Barlow, S.; Marder, S. R.; Perry, J. W. *J. Am. Chem. Soc.* **2006**, *128*, 11362–11363.

(18) Chung, S.; Zheng, S.; Odani, T.; Beverina, L.; Fu, J.; Padilha, L. A.; Biesso, A.; Hales, J. M.; Zhan, X.; Schmidt, K.; et al. *J. Am. Chem. Soc.* **2006**, *128*, 14444–14445.

(19) Balaz, M.; Collins, H. A.; Dahlstedt, E.; Anderson, H. L. *Org. Biomol. Chem.* **2009**, *7*, 874–888.

(20) Drobizhev, M.; Tillo, S.; Makarov, N. S.; Hughes, T. E.; Rebane, A. *J. Phys. Chem. B* **2009**, *113*, 855–859.

(21) Mikhail, D.; Yuriy, S.; Yuliya, D.; Aliaksandr, K.; Aleksander, R.; Taylor, P. N.; Anderson, H. L. *J. Phys. Chem. B* **2005**, *109*, 7223–7236.

(22) Suk, K. K.; Bum, N. S.; Takayuki, K.; Shuji, I.; Atsuhiro, O.; Dongho, K. *Chem. Commun.* **2007**, *24*, 2479–2481.

(23) Liu, Z.; et al. *J. Opt. Soc. Am. B* **2007**, *24*, 1101–1104.

Chart 1. Chemical Structures of Phosphine-Substituted Terthiophenes

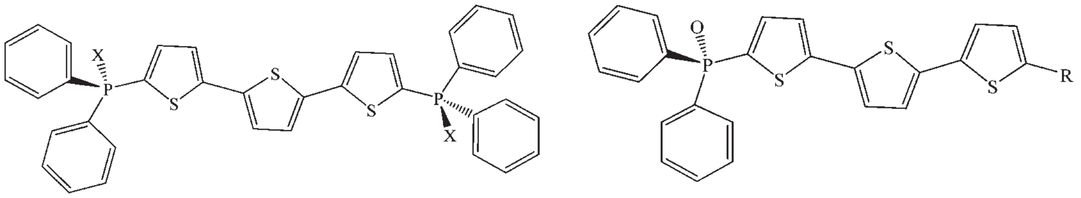

X = O **2**; X = S **3**; X = MeI **4**

R = H **6**; R = CHO **7**; R = CH_2OH **8**;

R = COOH **9**; R = CO_2Me **10**;

R = HC(N)Ph **11**

Polythiophene-derived compounds possessing extended π-conjugated networks and large concentrations of easily polarizable electrons are one class of materials that exhibit promising third-order nonlinear optical behavior.[24,25] Functionalization of short conjugated oligothiophenes can change the third-order nonlinear optical properties of the compounds and may also increase their solubilities, allowing solutions with high concentrations to be prepared to maximize the macroscopic nonlinearity of the bulk solution.[26−28] In our first paper in this area, we demonstrated that some transition metal complexes with diphenylphosphino-2,2′-terthiophene ligands exhibited nonlinear optical absorption at 532 nm and that the nature of the metal center affects the strength of the NLA.[29] However, the fact that this wavelength is significantly removed from the linear absorption maxima of the complexes suggests that better NLA might be observed at wavelengths closer to the linear absorption maxima, especially if excited state absorption is a major contributor to the NLA.

In this paper, we report the syntheses of two families of phosphine-substituted terthiophenes shown in Chart 1. The first family consists of disubstituted terthiophenes derived from 5,5″-bis(diphenylphosphino)-2,2′:5′,2″-terthiophene (PT_3P), and the second family consists of monosubstituted terthiophenes derived from 5-(diphenylphosphino)-2,2′:5′,2″-terthiophene (PT_3). The linear optical properties of the compounds have been evaluated using both UV−vis and fluorescence spectroscopy, and the nonlinear optical properties have been evaluated using NLA measurements with picosecond laser pulses in the blue region near the absorption maxima of the compounds.

Experimental Section

Materials. All reagents were reagent grade quality, purchased commercially, and used as such unless otherwise indicated. Urea hydrogen peroxide (1 g tablets) was purchased from Acros Organics. Tetrahydrofuran (THF) was dried over $MgSO_4$, refluxed over sodium/benzophenone and then distilled prior to use. Dry 1,2-dichloroethane and chloroform were prepared by refluxing the liquids over CaH_2 for several hours followed by distillation. Compounds **1** and **5** were prepared using literature procedures.[30]

Spectroscopic Characterization. One-dimensional multinuclear ^1H, $^{31}P\{^1H\}$, and $^{13}C\{^1H\}$ NMR spectra were recorded on a Bruker DRX-400 NMR spectrometer. The $^{31}P\{^1H\}$ NMR spectra were referenced to external 85% phosphoric acid (H_3PO_4) in a coaxial tube that also contained chloroform-*d*. The ^1H NMR and $^{13}C\{^1H\}$ NMR spectra were referenced to internal tetramethylsilane (TMS). Two-dimensional COSY (Correlated Spectroscopy), HSQC (Heteronuclear Single Quantum Coherence Spectroscopy), and HMBC (Heteronuclear Multiple Bond Correlation) were recorded on a Bruker DPX-300 NMR spectrometer. Electrospray ionization mass spectrometry (ESI MS) was performed on a MicroMass Platform LCZ instrument. Linear absorption spectra were recorded on a Varian Cary-100 UV−visible spectrophotometer. Microanalyses for % C and H were performed by Atlantic Microlab, Inc.

5,5″-Bis(diphenyloxophosphino)-2,2′:5′,2″-terthiophene, $Ph_2(O)P(C_4H_2S)_3P(O)Ph_2$, 2. Compound **2** was prepared by a modification of a previous procedure.[31] Excess H_2O_2-urea pellets (4.0 g) were added to a solution of **1** (1.00 g, 1.62 mmol) in CH_3OH (200 mL). The reaction mixture was stirred at room temperature overnight and then was evaporated to dryness under reduced pressure to yield a solid residue. The residue was purified by column chromatography (hexanes-ethyl acetate, 1:3 v/v) to yield the analytically pure product as a yellow crystalline solid (0.70 g, 66%). ESI-MS: 648.7 [M^+]. $^{31}P\{^1H\}$ NMR ($CDCl_3$): 23.42 (s). $^{13}C\{^1H\}$ NMR ($CDCl_3$): δ 145.13 (d, $|^3J_{CP}|$ 5.4 Hz, $C_{Th\text{-}2}$), 137.70 (d, $|^2J_{CP}|$ 8.9 Hz, $C_{Th\text{-}4}$), 136.07 (d, $|^4J_{CP}|$ 1.6 Hz, $C_{Th\text{-}2'}$), 132.73 (d, $|^1J_{CP}|$ 110.6 Hz, $C_{Th\text{-}5}$), 132.44 (d, $|^1J_{CP}|$ 110.3 Hz, $C_{Ph\text{-}i}$), 132.37 (d, $|^4J_{CP}|$ 2.8 Hz, $C_{Ph\text{-}p}$), 131.58 (d, $|^2J_{CP}|$ 10.4 Hz, $C_{Ph\text{-}o}$), 128.62 (d, $|^3J_{CP}|$ 12.7 Hz, $C_{Ph\text{-}m}$), 125.97 (s, $C_{Th\text{-}3'}$), 124.80 (d, $|^3J_{CP}|$ 12.8 Hz, $C_{Th\text{-}3}$). ^1H NMR ($CDCl_3$): 7.73−7.67 (m, 8H, $H_{Ph\text{-}o}$), 7.47−7.43 (m, 4H, $H_{Ph\text{-}p}$), 7.39−7.35 (m, 8H, $H_{Ph\text{-}m}$), 7.29 (dd, 2H, $|^3J_{PH}|$ 7.5 Hz, $|^3J_{HH}|$ 3.7 Hz, $H_{Th\text{-}4}$), 7.15 (dd, 2H, $|^3J_{HH}|$ 3.7 Hz, $|^4J_{PH}|$ 1.9 Hz, $H_{Th\text{-}3}$), 7.03 (s, 2H, $H_{Th\text{-}3'}$). UV−vis (CH_2Cl_2): λ_{max}/nm (ε/dm$^3\cdot$mol$^{-1}\cdot$cm^{-1}) = 373 (20300). Anal. Calcd for [$C_{36}H_{26}O_2P_2S_3$ H_2O]: C, 64.85; H, 4.20. Found: C, 64.50; H, 4.09.

5,5″-Bis(diphenylsulfidophosphino)-2,2′:5′,2″-terthiophene, $Ph_2(S)P(C_4H_2S)_3P(S)Ph_2$, 3. Excess elemental sulfur (0.30 g) was added to a solution of **1** (0.40 g, 0.65 mmol) in CH_2Cl_2 (50 mL). The reaction mixture was stirred at room temperature overnight, and then was evaporated under reduced pressure to give a solid residue. The residue was purified by column chromatography. First elution with hexanes removed the excess sulfur and then elution with Et_2O yielded the analytically pure product as a yellow crystalline solid

---

(24) Roncali, J. *Chem. Rev.* **1992**, *92*, 711–738.

(25) Dodabalapur, A.; Bao, Z.; Makhija, A.; Laquindanum, J. G.; Raju, V. R.; Fenf, Y.; Katz, H. E.; Rogers, J. *Appl. Phys. Lett.* **1998**, *73*, 142–144.

(26) Bednarz, M.; Reineker, P.; Mena-Osteritz, E.; Bäuerle, P. *J. Lumin.* **2004**, *110*, 225–231.

(27) Bidan, G.; Nicola, A. D.; Enĕe, V.; Guillerez, S. *Chem. Mater.* **1998**, *10*, 1052–1058.

(28) Krömer, J.; Bäuerle, P. *Tetrahedron* **2001**, *57*, 3785–3794.

(29) Myrex, R. D.; Gray, G. M.; Spivey, A. G. V.; Lawson, C. M. *Organometallics* **2006**, *25*, 5045–5050.

(30) Field, J. S.; Haines, R. J.; Lakoba, E. I.; Sosabowski, M. H. *J. Chem. Soc., Perkin Trans. I* **2001**, 3352–3360.

(31) Clot, O.; Akahori, Y.; Moorlag, C.; Leznoff, D. B.; Wolf, M. O.; Batchelor, R. J.; Patrick, B.; Ishii, O. M. *Inorg. Chem.* **2003**, *42*, 2704–2713.

(0.25 g, 60%). ESI-MS: 681.3. $^{31}\mathrm{P}\{^{1}\mathrm{H}\}$ NMR ($CDCl_3$): 34.64 (s). $^{13}\mathrm{C}\{^{1}\mathrm{H}\}$ NMR ($CDCl_3$): δ 145.47 (d, $|^{3}J_{\text{CP}}|$ 5.1 Hz, $C_{\text{Th-2}}$), 137.66 (d, $|^{2}J_{\text{CP}}|$ 8.7 Hz, $C_{\text{Th-4}}$), 136.13 (d, $|^{4}J_{\text{CP}}|$ 1.6 Hz, $C_{\text{Th-2}'}$), 134.32 (d, $|^{1}J_{\text{CP}}|$ 92.1 Hz, $C_{\text{Th-5}}$), 133.22 (d, $|^{1}J_{\text{CP}}|$ 89.6 Hz, $C_{\text{Ph-i}}$), 131.92 (d, $|^{4}J_{\text{CP}}|$ 3.0 Hz, $C_{\text{Ph-}p}$), 131.78 (d, $|^{2}J_{\text{CP}}|$ 11.3 Hz, $C_{\text{Ph-}o}$), 128.62 (d, $|^{3}J_{\text{CP}}|$ 13.1 Hz, $C_{\text{Ph-}m}$), 125.92 (s, $C_{\text{Th-3}'}$), 124.77 (d, $|^{3}J_{\text{CP}}|$ 12.9 Hz, $C_{\text{Th-3}}$). ^{1}H NMR ($CDCl_3$): 7.82−7.76 (m, 8H, $H_{\text{Ph-}o}$), 7.54−7.45 (m, 12H, $H_{\text{Ph-}p\text{ and }m}$), 7.32−7.26 (dd, 2H, $|^{3}J_{\text{PH}}|$ 8.2 Hz, $|^{3}J_{\text{HH}}|$ 3.8 Hz, $H_{\text{Th-4}}$), 7.18−7.16 (dd, 2H, $|^{3}J_{\text{HH}}|$ 3.8 Hz, $|^{4}J_{\text{PH}}|$ 1.8 Hz, $H_{\text{Th-3}}$), 7.10 (s, 2H, $H_{\text{Th-3}'}$). UV−vis (CH_2Cl_2): $\lambda_{\max}$/nm (ε/dm$^{3}\cdot$mol$^{-1}\cdot$cm^{-1}) = 377 (19300). Anal. Calcd for [$C_{36}H_{26}P_2S_5$]: C, 63.51; H, 3.85. Found: C, 63.06; H, 4.19.

5,5″-Bis(diphenylmethylphosphino)-2,2′:5′,2″-terthiophene Iodide, [$Ph_2(Me)P(C_4H_2S)_3P(Me)Ph_2]I_2$, 4. Excess CH_3I (1.0 mL) was added to a solution of **1** (0.30 g, 0.49 mmol) in CH_2Cl_2 (30 mL). The reaction mixture was stirred at room temperature overnight and then was evaporated under reduced pressure to give a yellow solid residue. Recrystallization from CH_3CN/Et_2O yielded the analytically pure product as a yellow crystalline solid (0.35 g, 80%). $^{31}\mathrm{P}\{^{1}\mathrm{H}\}$ NMR (CD_3CN): 16.97 (s). $^{13}\mathrm{C}\{^{1}\mathrm{H}\}$ NMR (CD_3CN): δ 148.66 (d, $|^{3}J_{\text{CP}}|$ 5.7 Hz, $C_{\text{Th-2}}$), 142.73 (d, $|^{2}J_{\text{CP}}|$ 9.6 Hz, $C_{\text{Th-4}}$), 135.33 (d, $|^{4}J_{\text{CP}}|$ 1.9 Hz, $C_{\text{Th-2}'}$), 135.09 (d, $|^{4}J_{\text{CP}}|$ 3.1 Hz, $C_{\text{Ph-}p}$), 132.67 (d, $|^{2}J_{\text{CP}}|$ 11.5 Hz, $C_{\text{Ph-}o\text{ or }m}$), 129.84 (d, $|^{3}J_{\text{CP}}|$ 13.4 Hz, $C_{\text{Ph-}m\text{ or }o}$), 127.97 (s, $C_{\text{Th-3}'}$), 126.86 (d, $|^{3}J_{\text{CP}}|$ 13.9 Hz, $C_{\text{Th-3}}$), 119.39 (d, $|^{1}J_{\text{CP}}|$ 92.0 Hz, $C_{\text{Th-5}}$), 116.13 (d, $|^{1}J_{\text{CP}}|$ 103.8 Hz, $C_{\text{Ph-i}}$), 9.88 (d, $|^{1}J_{\text{CP}}|$ 59.1 Hz, C_{CH3}). ^{1}H NMR (CD_3CN): 7.95−7.90 (m, 4H, H_{Ph} and $H_{\text{Th-4}}$), 7.87−7.74 (m, 18H, H_{Ph}), 7.67−7.65 (dd, 2H, $|^{3}J_{\text{HH}}|$ 4.0 Hz, $|^{4}J_{\text{PH}}|$ 2.2 Hz, $H_{\text{Th-3}}$), 7.47 (s, 2H, $H_{\text{Th-3}'}$), 2.96 (d, 6H, $|^{2}J_{\text{PH}}|$ 14 Hz, H_{CH3}). UV−vis (CH_3CN): $\lambda_{\max}$/nm (ε/dm$^{3}\cdot$mol$^{-1}\cdot$cm^{-1}) = 387 (35500). Anal. Calcd for [$C_{38}H_{32}P_2S_3I_2\ H_2O$]: C, 49.68; H, 3.73. Found: C, 49.60; H, 3.60.

5-(Diphenyloxophosphino)-2,2′:5′,2″-terthiophene, $Ph_2(O)P(C_4H_2S)_3H$, 6. Excess H_2O_2-urea pellets (4.0 g) were added to a solution of **5** (1.32 g, 3.05 mmol) in CH_3OH (300 mL). The reaction mixture was stirred at room temperature overnight and then was evaporated to dryness under reduced pressure to give a solid residue. This residue was purified by column chromatography (Et_2O eluent) to yield the analytically pure product as a yellow crystalline solid (1.15 g, 85.1%). ESI-MS: 449.0 [M^{+}]. $^{31}\mathrm{P}\{^{1}\mathrm{H}\}$ NMR ($CDCl_3$): 22.65 (s). $^{13}\mathrm{C}\{^{1}\mathrm{H}\}$ NMR ($CDCl_3$): δ 145.73 (d, $|^{3}J_{\text{CP}}|$ 5.3 Hz, $C_{\text{Th-2}}$), 137.93 (s, $C_{\text{Th-5}'\text{ or }2''}$), 137.73 (d, $|^{2}J_{\text{CP}}|$ 8.9 Hz, $C_{\text{Th-4}}$), 136.64 (s, $C_{\text{Th-5}'\text{ or }2''}$), 134.39 (d, $|^{4}J_{\text{CP}}|$ 1 Hz, $C_{\text{Th-2}'}$), 132.62 (d, $|^{1}J_{\text{CP}}|$ 110.2 Hz, $C_{\text{Ph-i}}$), 132.01 (d, $|^{1}J_{\text{CP}}|$ 111.6 Hz, $C_{\text{Th-5}}$), 132.31 (d, $|^{4}J_{\text{CP}}|$ 2.8 Hz, $C_{\text{Ph-}p}$), 131.83 (d, $|^{2}J_{\text{CP}}|$ 10.4 Hz, $C_{\text{Ph-}o}$), 128.59 (d, $|^{3}J_{\text{CP}}|$ 12.7 Hz, $C_{\text{Ph-}m}$), 127.98 (s, $C_{\text{Th-4}''}$), 125.86 (s, $C_{\text{Th-3}'\text{ or }4'}$), 125.01 (s, $C_{\text{Th-3}''\text{ or }5''}$), 124.45 (s, $C_{\text{Th-3}'\text{ or }4'}$), 124.33 (d, $|^{3}J_{\text{CP}}|$ 12.8 Hz, $C_{\text{Th-3}}$), 124.15 (s, $C_{\text{Th-3}''\text{ or }5''}$). ^{1}H NMR ($CDCl_3$): 7.80−7.75 (m, 4H, $H_{\text{Ph-}o}$), 7.58−7.56 (m, 2H, $H_{\text{Ph-}p}$), 7.52−7.47 (m, 4H, $H_{\text{Ph-}m}$), 7.36 (dd, 1H, $|^{3}J_{\text{PH}}|$ 7.5 Hz, $|^{3}J_{\text{HH}}|$ 3.8 Hz, $H_{\text{Th-4}}$), 7.25 (dd, 1H, $|^{3}J_{\text{HH}}|$ 5.1 Hz, $|^{4}J_{\text{HH}}|$ 1.1 Hz, $H_{\text{Th-3}''\text{ or }5''}$), 7.21 (dd, 1H, $|^{4}J_{\text{PH}}|$ 1.9 Hz, $|^{3}J_{\text{HH}}|$ 3.8 Hz, $H_{\text{Th-3}}$), 7.19 (m, 1H, $H_{\text{Th-3}''\text{ or }5''}$), 7.13 (d, 1H, $|^{3}J_{\text{HH}}|$ 3.8 Hz, $H_{\text{Th-3}'\text{ or }4'}$), 7.08 (d, 1H, $|^{3}J_{\text{HH}}|$ 3.8 Hz, $H_{\text{Th-3}'\text{ or }4'}$), 7.03 (dd, 1H, $|^{3}J_{\text{HH}}|$ 5.1 Hz, $|^{3}J_{\text{HH}}|$ 3.6 Hz, $H_{\text{Th-4}''}$). UV−vis (CH_2Cl_2): $\lambda_{\max}$/nm (ε/dm$^{3}\cdot$mol$^{-1}\cdot$cm^{-1}) = 368 (20500). Anal. Calcd for [$C_{24}H_{17}OPS_3$]: C, 64.26; H, 3.82. Found: C, 64.50; H, 4.01.

5-(Diphenyloxophosphino)-2,2′:5′,2″-terthiophene-5″-carbaldehyde, $Ph_2(O)P(C_4H_2S)_3CHO$, 7. Compound **6** (0.55 g, 1.2 mmol) was dissolved in 50 mL of dry 1,2-dichloroethane under nitrogen atmosphere. Excess DMF (2.0 mL) was first added to this solution and then $POCl_3$ (0.60 mL, 6.6 mmol) was added dropwise with stirring. The reaction mixture was heated at 60 °C under nitrogen for 36 h and then was poured slowly into 100 mL of saturated aqueous sodium acetate solution. This mixture was stirred for 2 h, and then the organic layer was diluted with CH_2Cl_2, separated, and washed with water. After evaporation of the solvents, the solid residue was purified with silica gel flash chromatography (hexanes−ethyl acetate 1:1) to yield the analytically pure product as a yellow product (0.50 g, 86%). ESI-MS: 476.9. $^{31}\mathrm{P}\{^{1}\mathrm{H}\}$ NMR ($CDCl_3$): 22.29 (s). $^{13}\mathrm{C}\{^{1}\mathrm{H}\}$ NMR ($CDCl_3$): δ 182.40 (s, C_{CHO}), 146.14 (s, $C_{\text{Th-5}''}$), 144.80 (d, $|^{3}J_{\text{CP}}|$ 5.3 Hz, $C_{\text{Th-2}}$), 142.04 (s, $C_{\text{Th-2}'\text{ or }5'\text{ or }2''}$), 137.67 (d, $|^{2}J_{\text{CP}}|$ 8.9 Hz, $C_{\text{Th-4}}$), 137.31 (s, $C_{\text{Th-3}''}$), 137.27 (s, $C_{\text{Th-2}'\text{ or }5'\text{ or }2''}$), 136.10 (s, $C_{\text{Th-2}'\text{ or }5'\text{ or }2''}$), 133.34 (d, $|^{1}J_{\text{CP}}|$ 110.0 Hz, $C_{\text{Th-5}}$), 132.49 (d, $|^{1}J_{\text{CP}}|$ 110.2 Hz, $C_{\text{Ph-i}}$), 132.40 (d, $|^{4}J_{\text{CP}}|$ 2.7 Hz, $C_{\text{Ph-}p}$), 131.80 (d, $|^{2}J_{\text{CP}}|$ 10.4 Hz, $C_{\text{Ph-}o}$), 128.63 (d, $|^{3}J_{\text{CP}}|$ 12.7 Hz, $C_{\text{Ph-}m}$), 126.95 (s, $C_{\text{Th-3}'\text{ or }4'}$), 126.14 (s, $C_{\text{Th-4}''}$), 125.12 (d, $|^{3}J_{\text{CP}}|$ 12.7 Hz, $C_{\text{Th-3}}$), 124.51 (s, $C_{\text{Th-3}'\text{ or }4'}$). ^{1}H NMR ($CDCl_3$): 9.87 (1H, s, H_{CHO}), 7.81−7.74 (4H, m, $C_{\text{Ph-}o}$), 7.68 (1H, d, $|^{3}J_{\text{HH}}|$ 3.8 Hz, $H_{\text{Th-3}''}$), 7.61−7.59 (2H, m, $C_{\text{Ph-}p}$), 7.53−7.50 (4H, m, $C_{\text{Ph-}m}$), 7.35 (1H, dd, $|^{3}J_{\text{PH}}|$ 7.5 Hz, $|^{3}J_{\text{HH}}|$ 3.8 Hz, $H_{\text{Th-4}}$), 7.28−7.17 (3H, m, $H_{\text{Th-3}}$ and $H_{\text{Th-3}'}$ and $H_{\text{Th-4}'}$), 7.17 (1H, d, $|^{3}J_{\text{HH}}|$ 3.8 Hz, $H_{\text{Th-4}''}$). UV−vis (CH_2Cl_2): $\lambda_{\max}$/nm (ε/dm$^{3}\cdot$mol$^{-1}\cdot$cm^{-1}) = 401 (37000). Anal. Calcd for [$C_{25}H_{17}O_2PS_3$]: C, 63.01; H, 3.60. Found: C, 62.79; H, 3.67.

5″-Hydroxymethyl-5-(diphenyloxophosphino)-2,2′:5′,2″-terthiophene, $Ph_2(O)P(C_4H_2S)_3CH_2OH$, 8. Sodium borohydride (0.010 g, 0.26 mmol) was added to a stirred solution of **7** (0.050 g, 0.10 mmol) in 10 mL of dry THF under nitrogen at ambient temperature. The reaction mixture was stirred overnight and then the THF was evaporated, water was added, and the mixture was stirred for 1 h. The resultant yellow precipitate was collected by filtration, and dried. Recrystallization from hexanes-ethyl acetate afforded the analytically pure product as yellow crystals (0.045 g, 90%). ESI-MS: 478.9. $^{31}\mathrm{P}\{^{1}\mathrm{H}\}$ NMR ($CDCl_3$): 23.04 (s). $^{13}\mathrm{C}\{^{1}\mathrm{H}\}$ NMR ($CDCl_3$): δ 145.80 (d, $|^{3}J_{\text{CP}}|$ 5.5 Hz, $C_{\text{Th-2}}$), 144.50 (s, $C_{\text{Th-5}''}$), 138.01 (s, $C_{\text{Th-2}'\text{ or }5'\text{ or }2''}$), 137.78 (d, $|^{2}J_{\text{CP}}|$ 9.1 Hz, $C_{\text{Th-4}}$), 136.50 (s, $C_{\text{Th-2}'\text{ or }5'\text{ or }2''}$), 134.28 (s, $C_{\text{Th-2}'\text{ or }5'\text{ or }2''}$), 132.44 (d, $|^{1}J_{\text{CP}}|$ 110.0 Hz, $C_{\text{Ph-i}}$), 132.35 (d, $|^{4}J_{\text{CP}}|$ 2.7 Hz, $C_{\text{Ph-}p}$), 131.70 (d, $|^{1}J_{\text{CP}}|$ 110.7 Hz, $C_{\text{Th-5}}$), 131.81 (d, $|^{2}J_{\text{CP}}|$ 10.4 Hz, $C_{\text{Ph-}o}$), 128.61 (d, $|^{3}J_{\text{CP}}|$ 12.7 Hz, $C_{\text{Ph-}m}$), 125.89 (s, $C_{\text{Th-4}''\text{ or }3'\text{ or }4'}$), 125.87 (s, $C_{\text{Th-4}''\text{ or }3'\text{ or }4'}$), 124.28 (d, $|^{3}J_{\text{CP}}|$ 12.8 Hz, $C_{\text{Th-3}}$), 124.25 (s, $C_{\text{Th-4}'\text{ or }3''}$), 123.70 (s, $C_{\text{Th-4}'\text{ or }3''}$), 60.02 (s, C_{CH2}). ^{1}H NMR ($CDCl_3$): 7.78−7.73 (4 H, m, $H_{\text{Ph-}o}$), 7.62−7.56 (2H, m, $H_{\text{Ph-}p}$), 7.51−7.48 (4H, m, $H_{\text{Ph-}m}$), 7.26 (1H, dd, $|^{3}J_{\text{PH}}|$ 7.8 Hz, $|^{3}J_{\text{HH}}|$ 3.8 Hz, $H_{\text{Th-4}}$), 7.15 (1H, dd, $|^{4}J_{\text{PH}}|$ 1.9 Hz, $|^{3}J_{\text{HH}}|$ 3.8 Hz, $H_{\text{Th-3}}$), 7.05 (1H, d, $|^{3}J_{\text{HH}}|$ 3.9 Hz, $H_{\text{Th-3}'\text{ or }4'}$), 6.98 (2H, d, $|^{3}J_{\text{HH}}|$ 3.8 Hz, $H_{\text{Th-3}'\text{ or }4'}$ and $H_{\text{Th-3}''}$), 6.86 (1H, d, $|^{3}J_{\text{HH}}|$ 3.5 Hz, $H_{\text{Th-4}''}$), 4.80 (2H, s, H_{CH2}). UV−vis (CH_2Cl_2): $\lambda_{\max}$/nm (ε/dm$^{3}\cdot$mol$^{-1}\cdot$cm^{-1}) = 377 (21300). Anal. Calcd for [$C_{25}H_{19}O_2PS_3$]: C, 62.74; H, 4.00. Found: C, 62.28; H, 3.91.

5-(Diphenyloxophosphino)-2,2′:5′,2″-terthiophene-5″-carboxylic Acid,$Ph_2(O)P(C_4H_2S)_3COOH$, 9. A mixture of Ag_2O (2.0 g, 8.6 mmol) in water (10 mL) was added to a solution of NaOH (1.0 g, 25 mmol) in water (10 mL) at room temperature. After this mixture was stirred for 15 min, a solution of **7** (0.20 g, 0.42 mmol) in THF (50 mL) was slowly added. The reaction mixture was stirred at room temperature for 0.5 h, and then was refluxed for 2 days. Next, the reaction mixture was acidified to pH = 4 with 10% aqueous HCl solution. The resulting brown precipitate was collected by filtration and washed with methanol. The filtrate and washings were combined and evaporated under reduced pressure to give a solid residue. The residue was purified by column chromatography with ethyl acetate as the eluent to yield the analytically pure product as an orange powder (0.12 g, 58%). ESI-MS: 492.9. $^{31}\mathrm{P}\{^{1}\mathrm{H}\}$ NMR (CD_3OD): 24.11 (s). ^{1}H NMR (CD_3OD): 7.09−7.03 (m. 4H, H_{Ph}), 6.99−6.97 (m, 3H, H_{Ph} and H_{Th}), 6.92−6.88 (m, 4H, H_{Ph}), 6.72−6.71 (m, 1H, H_{Th}), 6.68−6.66 (m, 1H, H_{Th}), 6.61−6.61(m, 2H, H_{Th}), 6.58−6.57 (m, 1H, H_{Th}).

Methyl 5-(diphenyloxophosphino)-2,2′:5′,2″-terthiophene-5″-carboxylate, $Ph_2(O)P(C_4H_2S)_3COOCH_3$, 10. Concentrated H_2SO_4 (1.0 mL) was added to a solution of **9** (0.10 g, 0.20 mmol) in methanol (100 mL). The reaction mixture was stirred under reflux overnight and then was evaporated under reduced pressure to give a solid residue. The residue was washed with water and then was purified by column chromatography (hexane-ethyl acetate, 1:1, v/v) to yield the analytically pure product as a yellow solid (0.095 g, 90%). ESI-MS: 506.9. $^{31}\mathrm{P}\{^{1}\mathrm{H}\}$ NMR ($CDCl_3$): 22.81 (s). $^{13}\mathrm{C}\{^{1}\mathrm{H}\}$ NMR ($CDCl_3$): δ 162.35 (s, $C_{\text{C=O}}$), 145.08 (d, $|^{3}J_{\text{CP}}|$ 5.5 Hz, $C_{\text{Th-2}}$), 143.24 (s, $C_{\text{Th-5}''}$), 137.69 (d, $|^{2}J_{\text{CP}}|$ 8.8 Hz, $C_{\text{Th-4}}$), 136.52 (s, $C_{\text{Th-5}'}$), 136.22 (d, $|^{4}J_{\text{CP}}|$ 1 Hz, $C_{\text{Th-2}'}$), 134.30 (s, $C_{\text{Th-3}''}$), 132.93 (d, $|^{1}J_{\text{CP}}|$

110.6 Hz, $C_{\text{Th-5}}$), 132.52 (d, $|^1J_{\text{CP}}|$ 110.1 Hz, $C_{\text{Ph-i}}$), 132.36 (d, $|^4J_{\text{CP}}|$ 2.7 Hz, $C_{\text{Ph-}p}$), 131.80 (d, $|^2J_{\text{CP}}|$ 10.4 Hz, $C_{\text{Ph-}o}$), 128.62 (d, $|^3J_{\text{CP}}|$ 12.7 Hz, $C_{\text{Ph-}m}$), 126.00 (s, $C_{\text{Th-3}'\text{ and }4'}$), 124.86 (d, $|^3J_{\text{CP}}|$ 12.7 Hz, $C_{\text{Th-3}}$), 124.22 (s, $C_{\text{Th-4}''}$), 52.30 (s, C_{CH3}). ^{1}H NMR ($CDCl_3$): 7.80−7.78 (m, 4H, $H_{\text{Ph-}o}$), 7.77 (d, 1H, $|^3J_{\text{HH}}|$ 3.9 Hz, $H_{\text{Th-3}''}$), 7.71−7.70 (m, 2H, $H_{\text{Ph-}p}$), 7.52−7.50 (m, 4H, $H_{\text{Ph-}m}$), 7.35 (dd, 1H, $|^3J_{\text{PH}}|$ 7.5 Hz, $|^3J_{\text{HH}}|$ 3.8 Hz, $H_{\text{Th-4}}$), 7.26 (dd, 1H, $|^4J_{\text{PH}}|$ 1.9 Hz, $|^3J_{\text{HH}}|$ 3.8 Hz, $H_{\text{Th-3}}$), 7.18 (d, 1H, $|^3J_{\text{HH}}|$ 3.8 Hz, $H_{\text{Th-4}'}$), 7.15 (d, 1H, $|^3J_{\text{HH}}|$ 3.8 Hz, $H_{\text{Th-3}'}$), 7.13 (d, 1H, $|^3J_{\text{PH}}|$ 3.8 Hz, $H_{\text{Th-4}''}$), 3.89 (s, 3H, H_{CH3}). UV−vis (CH_2Cl_2): $\lambda_{\max}$/nm (ε/dm$^3\cdot$mol$^{-1}\cdot$cm^{-1}) = 387 (12800). Anal. Calcd for [$C_{26}H_{19}O_3PS_3$]: C, 61.64; H, 3.78. Found: C, 61.66; H, 3.99.

5″-Phenyliminomethyl-5-(diphenyloxophosphino)-2,2′:5′,2″-terhiophene, $\mathbf{Ph_2(O)P(C_4H_2S)_3CHNPh}$, 11. A solution of **7** (0.050 g, 0.10 mmol) and aniline (40 μL, 4.38 mmol) in 10 mL of dry $CHCl_3$ was refluxed under nitrogen for 36 h. After evaporation of the solvents, the residue was purified with flash chromatography (CH_2Cl_2-ethyl acetate, 3:1, neutral aluminum oxide) to yield the analytically pure product as a yellow powder (0.050 g, 86%). ESI-MS: 551.9. ^{31}P{^{1}H} NMR ($CDCl_3$): 22.57 (s). ^{13}C{^{1}H} NMR ($CDCl_3$): δ 152.32 (s, $C_{\text{C=N}}$), 151.12 (s, $C_{\text{Th-5}'\text{ or }2''\text{ or }5''\text{ or NPh-i}}$), 145.28 (d, $|^3J_{\text{CP}}|$ 5.3 Hz, $C_{\text{Th-2}}$), 141.85 (s, $C_{\text{Th-5}'\text{ or }2''\text{ or }5''\text{ or NPh-i}}$), 141.04 (s, $C_{\text{Th-5}'\text{ or }2''\text{ or }5''\text{ or NPh-i}}$), 137.68 (d, $|^3J_{\text{CP}}|$ 8.6 Hz, $C_{\text{Th-3 or 4}}$), 137.24 (s, $C_{\text{Th-5}'\text{ or }2''\text{ or }5''\text{ or NPh-i}}$), 135.80 (d, $|^4J_{\text{CP}}|$ 1.6 Hz, $C_{\text{Th-2}'}$), 132.98 (d, $|^5J_{\text{CP}}|$ 2.1 Hz, $C_{\text{Th-3}'\text{ or }4'}$), 132.71 (d, $|^1J_{\text{CP}}|$ 113 Hz, $C_{\text{Th-5}}$), 132.57 (d, $|^1J_{\text{CP}}|$ 108 Hz, $C_{\text{PPh-i}}$), 132.34 (d, $|^4J_{\text{CP}}|$ 2.5 Hz, $C_{\text{PPh-}p}$), 131.81 (d, $|^2J_{\text{CP}}|$ 10.4 Hz, $C_{\text{PPh-}o}$), 129.18 (s, $C_{\text{NPh-o or NPh-m}}$), 128.61 (d, $|^3J_{\text{CP}}|$ 12.6 Hz, $C_{\text{PPh-}m}$), 126.22 (s, $C_{\text{Th-3}'\text{ or }4'}$), 126.09 (s, $C_{\text{Th-3}''\text{ or }4''}$), 125.74 (s, $C_{\text{Th-3}''\text{ or }4''}$), 124.73 (d, $|^2J_{\text{CP}}|$ 12.8 Hz, $C_{\text{Th-3 or 4}}$), 124.29 (s, $C_{\text{NPh-p}}$), 121.05 (s, $C_{\text{NPh-o or NPh-m}}$). ^{1}H NMR ($CDCl_3$): 8.44 (1H, s, $H_{\text{C=N}}$), 7.73−7.67 (4 H, m, H_{PPh}), 7.55−7.42 (6H, m, H_{PPh}), 7.35−7.28 (4H, m, H_{Th}), 7.28−7.07 (7H, m, $H_{\text{NPh and}}$ H_{Th}). UV−vis (CH_2Cl_2): $\lambda_{\max}$/nm (ε/dm$^3\cdot$mol$^{-1}\cdot$cm^{-1}) = 411 (47800). Anal. Calcd for [$C_{31}H_{22}NOPS_3$]: C, 67.49; H, 4.02. Found: C, 67.08; H, 4.10.

X-ray Data Collection and Solution. A suitable single crystal of **2** was glued on a glass fiber with epoxy and aligned upon an Enraf-Nonius CAD4 single-crystal diffractometer under aerobic conditions. Standard peak search and automatic indexing routines followed by least-squares fits of 25 accurately centered reflections resulted in accurate unit cell parameters. The space group of the crystal was assigned on the basis of systematic absences and intensity statistics. All data collections were carried out using the CAD4-PC software,[32] and details of the data collections are given in Table 1. The analytical scattering factors of the complex were corrected for both $\Delta f'$ and $i\Delta f''$ components of anomalous dispersion. All data were corrected for Lorentz and polarization effects.

All crystallographic calculations were performed with the Siemens SHELXTL-PC program package.[33] All heavy atom positions were located using Direct Methods. Full-matrix refinements of the positional and anisotropic thermal parameters for all non-hydrogen atoms versus F^2 were carried out. All hydrogen atoms were placed in calculated positions with the appropriate molecular geometry and δ (C−H) = 0.96 Å. The isotropic thermal parameter of each hydrogen atom was fixed equal to 1.2 times the U_{eq} value of the atom to which it was bound. Crystallographic data has been deposited with the Cambridge Crystallographic Database Centre (CCDC 773042).

Table 1. Data Collection Parameters for X-ray Structure Determination

identification code	**2**
empirical formula	C36 H28 O3 P2 S3
formula weight	666.70
temperature	293(2) K
wavelength	0.71073 Å
crystal system	monoclinic
space group	$C2/c$
unit cell dimensions	a = 18.327(4) Å
	b = 9.6335(19) Å
	c = 18.711(4) Å
	β = 103.74 (3)°
volume	3208.9(11) Å^3
Z	4
density (calculated)	1.380 Mg/m^3
absorption coefficient	0.367 mm^{-1}
F(000)	1384
crystal size	0.5 × 0.7 × 0.3 mm^3
θ range for data collection	2.24° to 22.48°
index ranges	$-10 \le h \le 19$
	$-10 \le k \le 9$
	$-20 \le l \le 19$
reflections collected	4840
independent reflections	2093 [R(int) = 0.0511]
absorption correction	None
refinement method	full-matrix least-squares on F^2
data/restraints/parameters	2093/0/230
goodness-of-fit on F^2	1.132
final R indices [$I > 2\sigma(I)$]	R1 = 0.0875
	wR2 = 0.2150
R indices (all data)	R1 = 0.1091
	wR2 = 0.2365
largest diff. peak and hole	1.034 and −0.456 e Å^{-3}

Solution Phase Fluorescence Measurements. Emission spectra in solution were obtained on a Cary Eclipse Fluorometer. Each of the compounds was freshly purified by chromatography before being used for the fluorescence measurements. Each solution was excited at the absorption wavelength maximum using a 10 mm path length quartz cell, and the concentrations used were 4.0 × 10^{-6} mol/L. All the fluorescence spectra were recorded with constant slit widths of 5 nm. All solutions were prepared using optima grade dichloromethane at room temperature, and the solutions were deoxygenated by bubbling N_2 through them for approximately 5 min.

The fluorescence intensity was approximately corrected according to the equation[34]

$$F_{\text{corr}}(\lambda) = F_{\text{obs}}(\lambda)\ \text{antilog}\left(\frac{\text{OD}_{\text{ex}} + \text{OD}_{\text{em}}}{2}\right) \qquad (1)$$

where $F_{\text{obs}}(\lambda)$ and $F_{\text{corr}}(\lambda)$ are the measured and corrected fluorescence intensities, respectively, OD_{ex} and OD_{em} are the optical densities at the excitation and the emission wavelength, respectively, assuming $\text{OD}_{\text{em}} = 0$. The integrated fluorescence intensity I (that is, the area of the fluorescence spectrum) was calculated using the equation

$$I = \int_a^b F_{\text{corr}}(\lambda)\, d\lambda \qquad (2)$$

where $F_{\text{corr}}(\lambda)$ is the corrected fluorescence spectrum on the wavelength scale, [a, b] is the finite range of wavelength, and $\Delta\lambda$ is the integration step (which is the band-pass). All the fluorescence spectra were recorded at the constant band-passes of 1.0 nm. It is straightforward to evaluate such integrals numerically. Among many numerical integration schemes, the trapezoidal rule to approximate the integral was adopted because of its simplicity and sufficient accuracy.[35]

The relative quantum yield for comparison with different samples was calculated using the equation[34]

$$\frac{Q}{Q_{\text{R}}} = \frac{I}{I_{\text{R}}}\,\frac{\text{OD}_{\text{R}}}{\text{OD}}\,\frac{n}{n_{\text{R}}} \qquad (3)$$

---

(32) *CAD4-PC*, Version 1.2; Enraf-Nonius: Delft, The Netherlands, 1988.

(33) Sheldrick, G. M. *SHELXTL NT*, Version 6.12; Bruker AXS, Inc.: Madison, WI, 2001.

(34) Lakowicz, J. R. *Principles of Fluorescence Spectroscopy*, 2nd ed.; Springer Science + Business Media Inc.: New York, 2004; Chapter 2.

(35) Atkinson, K.E. *An Introduction to Numerical Analysis*, 2nd ed., John Wiley & Sons: New York, 1989; Chapter 5.

Scheme 1. Synthesis of Compounds **2**, **3**, and **4** from $Ph_2P(C_4H_2S)_3PPh_2$ (**1**)

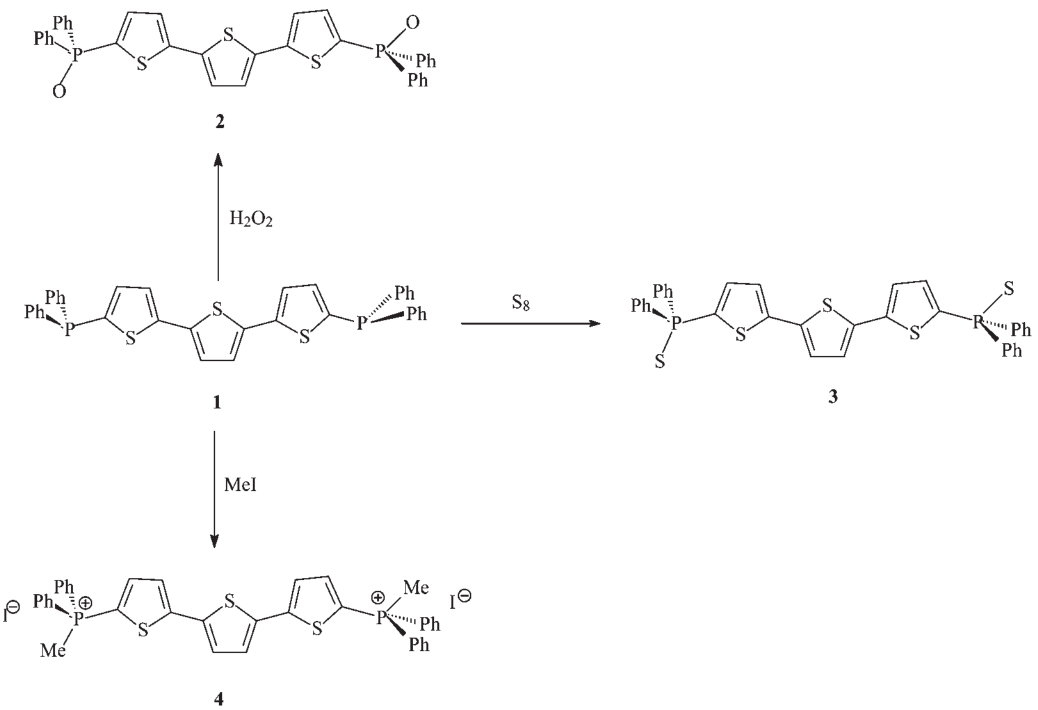

where Q is the quantum yield, I is the integrated intensity, OD is the optical density, and n is the refractive index of the solvent. The subscript R refers to the reference solution, which was a CH_2Cl_2 solution of terthiophene (T_3).

Thin Film and Single Molecule Fluorescence Measurements. Emissions from thin films composed of the disubstituted terthiophenes **2**, **3**, and **4** and from single disubstituted terthiophene molecules of **4** were measured using a Nikon TE-2000U inverted microscope. Molecules were deposited from dilute solutions (10^{-6} mol/L for thin films and 10^{-8} mol/L for single molecule measurements) in THF onto plasma-cleaned coverslips using the drop cast method. The 457 nm line from a Coherent Innova 200 Ar ion laser was employed to excite the samples as a function of laser power and fluorescence emission was detected using a Princeton Instruments Photonmax EMCCD camera. Typical CCD camera exposure times were 0.2 s. Solid state fluorescence spectra were obtained by dispersing the emitted light using a Princeton Instruments 2150 Spectrograph before detection.

Linear and Nonlinear Optical Transmission Measurements. Linear transmission measurements of dichloromethane solutions of the compounds (3.65×10^{-3} mol/L for **2**, **3**, and **10**; 3.5×10^{-3} mol/L for all other compounds) in a 1 mm cuvette were performed on a Shimadzu UV-3101PC Spectrophotometer. Nonlinear transmission measurements were performed at 450 nm, 480 and 532 nm on the same solutions in the same cuvette. A wavelength tunable laser system, consisting of an EKSPLA PG401 optical parametric generator (OPG) pumped by a PL2143A/ss model-locked Nd:YAG laser with a pulse width of 27 ps and a repetition rate of 10 Hz, was used as the light source. Laser radiation energy was gradually changed by using a motorized attenuator based on a combination of a half-wave plate and a Glan-Taylor prism. Part of the laser beam was then reflected by a beam splitter to a reference detector to monitor the incident energy. The remaining beam was focused by a 300 mm lens to the center of a 1 mm sample cell (Spectrosil 21-Q-1, Starna Cells, Inc.). The diameters of focused beam were 73, 80, and 97 μm at 450, 480, and 532 nm, respectively. The transmitted signal energy and the reference energy were monitored by two Molectron J4−09 pyroelectric joule meters.

Results and Discussion

Syntheses of Derivatives of 5,5″-Bis(diphenylphosphino)-2,2′:5′,2″-terthiophene. Bis(diphenenylphosphino)- and (diphenylphosphino)-substituted terthiophenes, **1** and **6**, were synthesized by lithiation of terthiophene followed by quenching with chlorodiphenylphosphine. Pure **6** was obtained in reasonably good yield (70%) by this synthetic approach, although Field et al. had previously reported that the selective monolithiation of terthiophene proved impossible using a wide range of stoichiometries and reaction conditions.[30] Compounds **2**, **3**, and **4** were synthesized by treating the free ligand **1** with hydrogen peroxide, elemental sulfur, and methyl iodide, respectively, as shown in Scheme 1. Compounds **2**−**4** were obtained in good yields and in high purities after workup by either column chromatography or recrystallization.

Functionalization of 5-(Diphenyloxophosphino)-2,2′:5′,2″-terthiophene at the 5″-Position. Oligothiophenes have been functionalized with a wide variety of organic functional groups to prepare molecular materials with a range of electrical and optical properties. Functional groups that have been incorporated into terthiophenes include aldehyde, carboxylic acid, methyl carboxylate, and hydroxymethyl groups.[36−41] However, no terthiophenes with both a phosphine substituent and one of these organic substituents have been reported. We have used modifications of the standard synthetic procedures to prepare terthiophenes with

---

(36) Wei, Y.; Wang, B.; Wang, W.; Tian, J. *Tetrahedron Lett.* **1995**, *36*, 665–668.

(37) Parakka, J. P.; Cava, M. P. *Tetrahedron* **1995**, *51*, 2229–2242.

(38) Skene, W. G.; Dufresne, S. *Org. Lett.* **2004**, *6*, 2949–2952.

(39) Kiriy, N.; Bocharova, V.; Kiriy, A.; Stamm, M.; Krebs, F. C.; Adler, H. *Chem. Mater.* **2004**, *16*, 4765–4771.

(40) Nakagawa, H.; Gomi, K.; Yamada, K. *Chem. Pharm. Bull.* **2001**, *49*, 49–53.

(41) Noguchi, T.; Hasegawa, M.; Tomisawa, K.; Mitsukuchi, M. *Bioorg. Med. Chem.* **2003**, *11*, 4729–4742.

Scheme 2. Functionalization of $Ph_2(O)P(C_4H_2S)_3H$ (**6**)

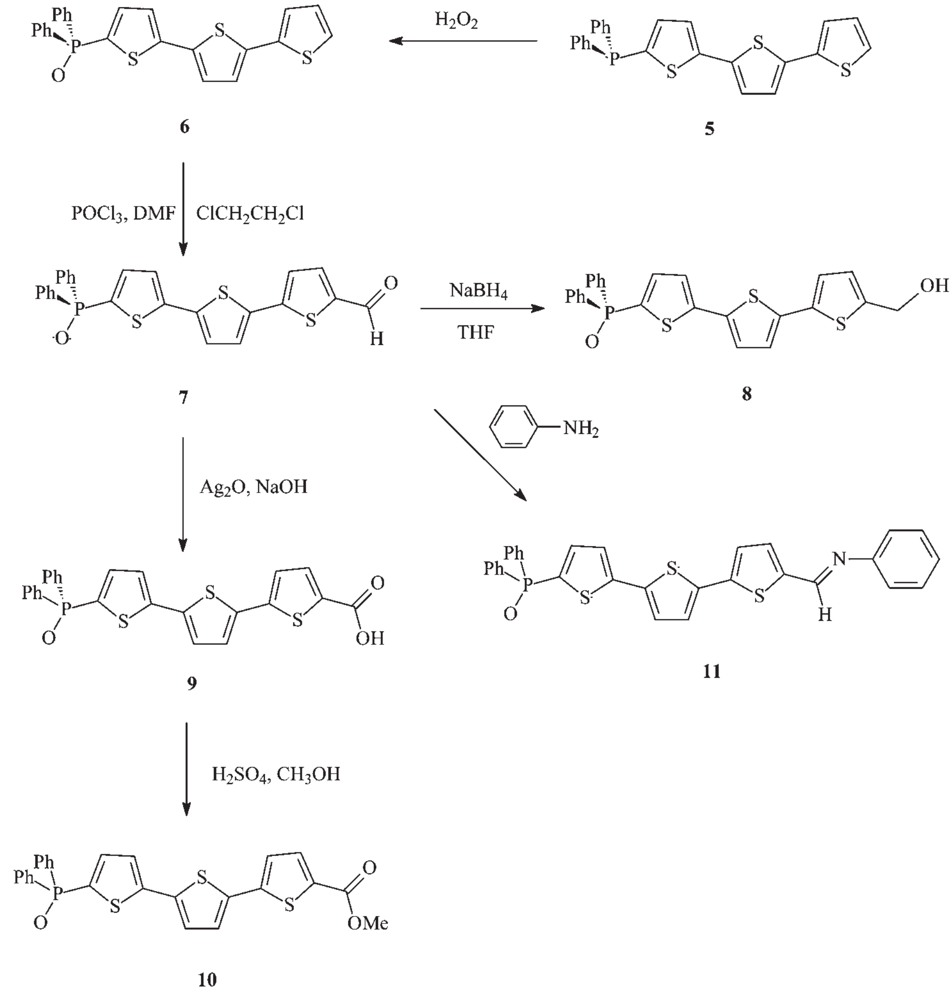

a diphenylphosphine oxide on the 5-position and an organic functional group at the 5″-position as shown in Scheme 2. As discussed below, the incorporation of an organic functional group has significant effects on the linear and nonlinear optical properties of the molecules. In addition, the functional groups may change inherent solubilities of chromophores or allow the chromophores to be attached to polymers.

NMR Spectroscopic Characterization. All the new compounds have been characterized by $^{31}P\{^1H\}$, $^{13}C\{^1H\}$, and ^1H NMR spectroscopy and mass spectroscopy. The mass spectra exhibited parent ions for the desired compounds in all cases. The $^{13}C\{^1H\}$ and ^1H NMR spectra are quite complicated and were assigned using a combination of two-dimensional COSY, HSQC, and HMBC techniques. In some cases it was not possible to uniquely assign all the resonances, and all possible assignments are indicated in the Experimental Section of this article.

The $^{31}P\{^1H\}$ NMR spectra are of particular interest because they provide insight into the factors that affect the electron density at the phosphorus. The resonances of **1** and **5** in $CDCl_3$ are singlets with very similar chemical shifts (−18.75 and −18.71 ppm, respectively) that are typical for diphenylphosphines with 2-thienyl substituents.[42] The $^{31}P\{^1H\}$ NMR resonances of compounds **2**, **3**, and **4** are also singlets but are considerably downfield compared to that of **1** (23.42, 34.64, and 16.97 ppm, respectively) indicating that coordination of the lone pair causes a significant downfield shift in the $^{31}P\{^1H\}$ NMR resonance. The $^{31}P\{^1H\}$ NMR resonance of **2**, in which an oxygen is coordinated to the phosphorus, is upfield of that of **3**, in which a sulfur is coordinated to the phosphorus. This indicates that the shifts in the $^{31}P\{^1H\}$ NMR resonances are not entirely due to the electron withdrawing abilities of the groups coordinated to the lone pair of the phosphorus. The chemical shifts of the ^{31}P NMR resonances of **2**, **3**, and **4** are quite similar to those of their bithiophene analogues, $Ph_2(X)P(C_4H_2S)_2P(X)Ph_2$ (X = O, 22.54 ppm; S, 34.64 ppm; CH_3^+ I^-, 17.73 ppm)[42] indicating that replacing a bithiophene with a terthiophene has no significant effect on the local magnetic field at the phosphorus atom.

The $^{31}P\{^1H\}$ NMR resonances of **6**−**8**, **10**, and **11** in $CDCl_3$ are singlets with chemical shifts between 22.09 and 23.04 ppm. Their chemical shifts are similar to one another and to that of **2** (23.42 ppm) even if the substituent extends the conjugation of the molecule. The similarities suggest that the substituent at the opposite end of the terthiophene has little effect on $^{31}P\{^1H\}$ NMR chemical shift, and hence on the electron density at the diphenylphosphine oxide group.

Single-Crystal X-ray Diffraction Analysis. We have previously reported the crystal structures for three bithiophene derivatives, $Ph_2(X)P(C_4H_2S)_2P(X)Ph_2$ in which X is O, S,

---

[42] Zhao, Q.; Owens, S. B., Jr.; Gray, G. M.; Wang, J.; Lawson, C. M. *Main Group Chem.* **2007**, *6*, 215–229.

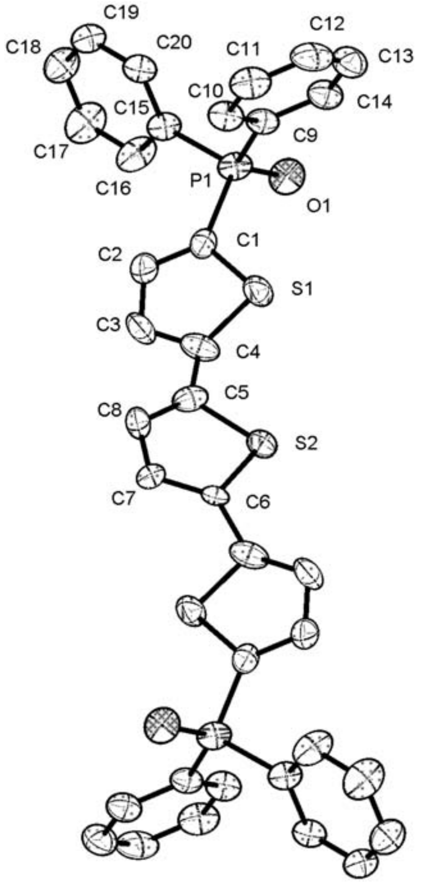

Figure 1. Molecular structure of **2** showing one orientation of the disordered central thiophene ring. Hydrogen atoms are omitted, and the atomic displacement ellipsoids are drawn at 25% probability.

and CH_3^+ I^-.[42] The most interesting feature of these structures was the extensive $\pi-\pi$ stacking that resulted in quite different orientations of the molecules in the crystals. The different orientations appeared to depend both on the crystallization conditions and on the X group. Thus, it is of interest to determine how replacing a bithiophene with a terthiophene affects the ability of the molecule to engage in $\pi-\pi$ stacking.

Crystals of compound **2** suitable for X-ray diffraction were obtained by slow diffusion of hexanes into a concentrated CH_2Cl_2 solution of the compound. Compound **2** crystallizes in the *C*2/*c* space group with the molecule occupying an inversion center. The center thiophene ring is thus disordered about this inversion center. The molecular structure of **2** is shown in Figure 1, and the selected bond lengths, bond angles, and torsion angles are given in Table 2.

The most interesting aspect of the crystal structure of **2** is the extensive $\pi-\pi$ stacking that is observed. Edge-to-face interactions are observed with all of the phenyl and thiophene rings as shown by the data in Table 3. Interactions are observed between phenyl a and two adjacent molecules of **2** and between phenyl b and one of the same adjacent molecules of **2** as well as another adjacent molecule of **2**. These interactions result in a tightly packed array in which molecules of **2** are located on the centers of each edge of the unit cell as well as on the centers of two opposite faces. The dihedral angles between the least-squares planes through the central, disordered thiophenes are zero, as shown in the drawing of the *ac* face of the unit cell in Figure 2a, but the molecules occupying the centers of the edges are rotated by (−53.8°) from those occupying the centers of the faces, as shown by the drawing of the *ab* face of the unit cell in Figure 2b.

Table 2. Selected Bond Lengths (Å), Bond Angles (deg), and torsion angles (deg) for **2**

C1−P1	1.857(7)
C9−P1	1.793(6)
O1−P1	1.467(5)
C15−P1	1.796(6)
O1−P1−C1	112.8(3)
O1−P1−C9	113.0(3)
O1−P1−C15	112.8(3)
S1−C4−C5−S2	−34.2(15)
S1−C1−P1−O1	59.3(4)
C14−C9−P1−O1	53.2(6)

Table 3. Intermolecular Edge to Face $\pi-\pi$ Interactions in the Crystal Structure of **2**

atom (ring)	centroid of ring[a]	distance (Å)
C11 (phenyl a)	phenyl b	3.938
C12 (phenyl a)	thiophene b	4.012
C13 (phenyl a)	phenyl b	3.676
C18 (phenyl b)	phenyl a	3.701
C20 (phenyl b)	thiophene a	3.941
C2 (thiophene a)	phenyl a	3.627

[a] Phenyl a is the phenyl comprised of C9−C14, phenyl b is the phenyl comprised of C15−C20, thiophene a is the thiophene comprised of S1 and C1−C4 and thiophene b is the thiophene comprised of S2 and C5−C8. Thiophene 2 is disordered about the inversion center, and the centroid for the two disordered rings is the inversion center.

A second feature of interest in the solid state structure of **2** is the planarity of the terthiophene group. Because of the location of the center of symmetry of **2**, this is measured only by the S(1)−C(4)−C(6)−S(2A) torsion angle. The significant deviation of this angle from 180° (157.5(6)°) may be a result of the $\pi-\pi$ stacking involving the thiophene rings.

The final feature of interest in the solid state structure of **2** is the orientation of the aromatic phosphorus substituents relative to the phosphorus−oxygen bond. The conformation about the phosphorus is a distorted tetrahedron with all of the O−P−C angles equal to one another and greater than the ideal angle of 109.5°. Orientations of the three aromatic substituents can be determined by comparing the S1−C1−P1−O1, C14−C9−P1−O1, and C16−C15−P1−O1 torsion angles (S1, O1, and C16 are the ortho ring atoms that are on the same side of the least-squares plane through C1, C9, and C14 as is the oxygen). The fact that all three torsion angles have positive signs means that the rings have a propeller orientation; however, the much larger C14−C9−P1−O1 torsion angle means that propeller orientation is distorted. It is of interest that the phosphorus−oxygen bond is nearly in the plane of one of the phenyl rings in **2** while in the structure of $Ph_2(O)P(C_4H_2S)_2P(O)Ph_2$, the phosphorus−oxygen bonds are nearly in the planes of the thienyl rings.[42]

Linear Absorption Spectra. Dichloromethane solutions of **2**−**8**, **10**, and **11** have an absorption band between 350 and 450 nm. The parent compounds **1** and **5** exhibit similar bands, and these bands have been assigned to $\pi \rightarrow \pi^*$ transitions on the basis of density functional calculations.[43]

---

(43) Stott, T. L.; Wolf, M. O. *J. Phys. Chem. B* **2004**, *108*, 188815–188819.

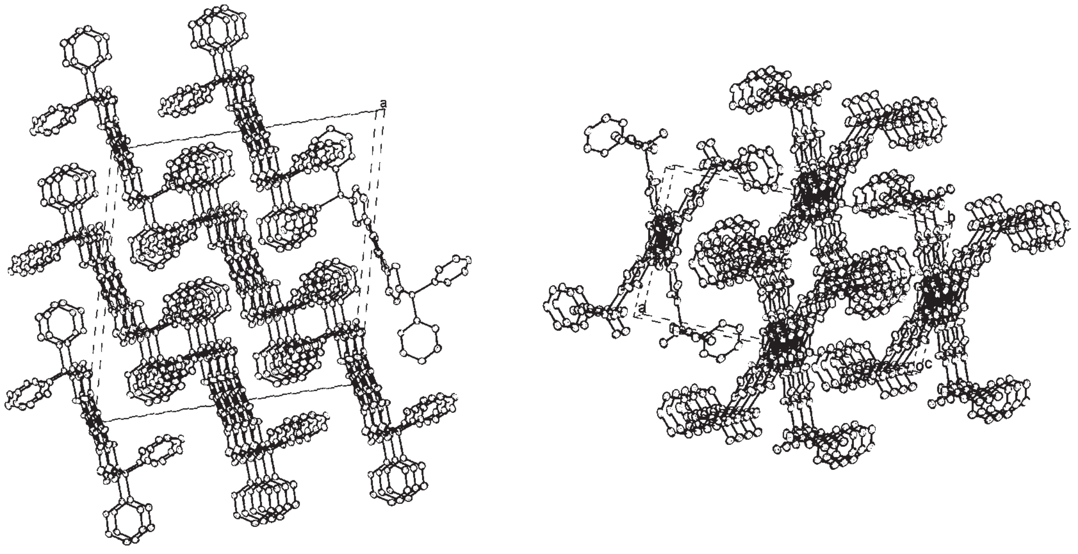

Figure 2. Left: *ac* face of the unit cell of **2**. Right: *ab* face of the unit cell of **2**.

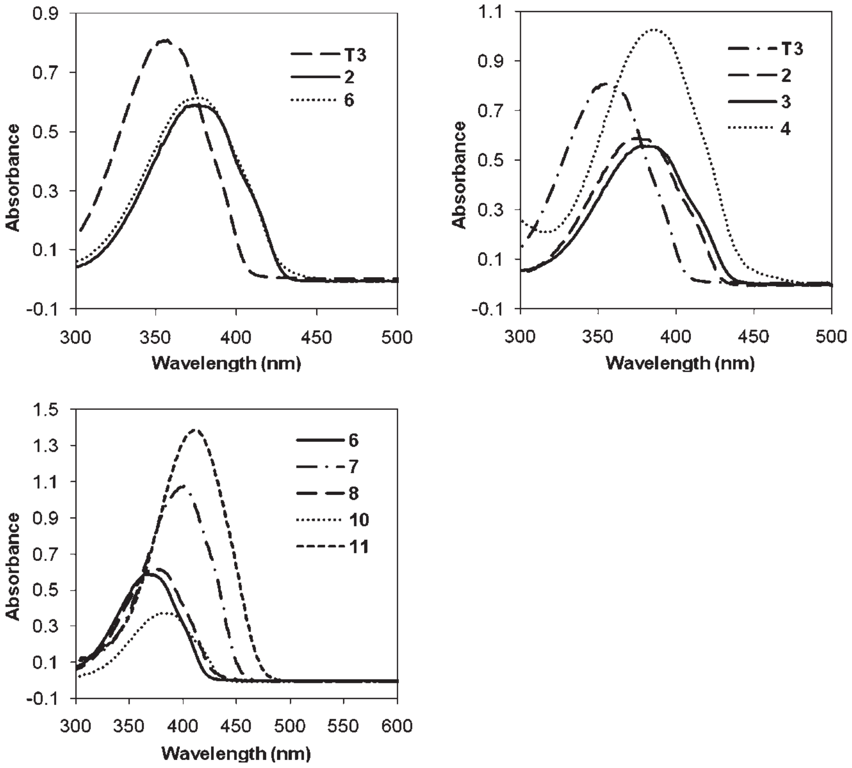

Figure 3. Linear absorption spectra in a 1-mm cell. Upper left: T_3, **2** and **6**; upper right: T_3, **2**, **3**, and **4**; bottom: **6**, **7**, **8**, **10**, and **11**. All solution concentrations are 2.9×10^{-4} mol/L in CH_2Cl_2. The solvent has negligible linear absorption in this spectral region.

As expected, the absorption maximum depends on the nature of the substituents on the terthiophene. Substitution of terthiophene with diphenyl(oxo)phosphino groups causes a red shift of 14 nm for each group (terthiophene: λ_{max} = 354 nm; **6**: λ_{max} = 368 nm; and **2**: λ_{max} = 382 nm) as shown in Figure 3a. This is consistent with the results of studies of related phosphine-substituted oligothiophenes and their amino analogues and has been rationalized as being due to stabilization of the lowest unoccupied molecular orbital via a bonding interaction with the phosphorus.[44,45]

Changing the group attached to the lone pair of electrons on the phosphorus has little effect on the absorption maximum (**2** (X = O): λ_{max} = 382 nm; **3** (X = S): λ_{max} = 382 nm; **4** (X = Me^+): λ_{max} = 387 nm). This is in contrast with previous results for the bithiophene compounds $Ph_2(X)P(C_4H_2S)_2P(X)Ph_2$ (X = O: λ_{max} = 326 nm; X = S: λ_{max} = 342 nm; X = Me^+: λ_{max} = 332 nm) but is consistent with results from density functional theory (DFT) calculations indicating that terthiophenes have little P character in their highest occupied and lowest unoccupied molecular orbitals.[43] It is of interest

---

(44) Tabet, A.; Schroder, A.; Hartmann, H.; Rohde, D.; Dunsch, L. *Org. Lett.* **2003**, *5*, 1817–1820.

(45) Changenet, P.; Plaza, P.; Martin, M. M.; Meyer, Y. H.; Rettig, W. *Chem. Phys.* **1997**, *221*, 311–322.

that although the substituent on the lone pair of electrons on the phosphorus does not affect the absorption maximum, it does affect the molar absorptivity with **2** (O) and **3** (S) having lower molar absorptivities than terthiophene and **4** (Me^+) having a higher molar absorptivity than terthiophene.

The linear absorption characteristics are very sensitive to the nature of the substituent at the 5″-position for the derivatives of the monophosphine **6**. A red shift is observed as more highly conjugated groups are introduced at the 5″-position (**6** (H): λ_{max} = 367 nm; **8** (CH_2OH): λ_{max} = 376 nm; **10** (CO_2Me): λ_{max} = 386 nm; **7** (CHO): λ_{max} = 398 nm; **11** (CH=NPh): λ_{max} = 411 nm) consistent with Woodward's Rules for conjugated carbonyl compounds.[46] The substituent at the 5″-position also affects the molar absorptivity with the most conjugated compounds exhibiting the highest molar absorptivities.

Solution Phase Fluorescence Spectra. The emission spectra were studied to gain additional insight into the nature of the first singlet excited state of the compounds in this photophysical study. For most fluorescent compounds, emission is produced by either a $\pi^* \rightarrow \pi$ or a $\pi^* \rightarrow n$ transition, depending on which of these is the less energetic. Empirically, $\pi \rightarrow \pi^*$ transitions are characterized by higher molar absorptivities and relatively higher fluorescence quantum yields than those of $n \rightarrow \pi^*$ transitions.[47] As previously reported by Wolf for the parent compounds **1** and **5**, the emission is attributed to a $\pi^* \rightarrow \pi$ transition.[43] DFT calculations, also reported by Wolf, supported this assignment by demonstrating that planarization does not occur at the phosphorus. In this case, the emission of the disubstituted terthiophene (λ_{em} = 465 nm) was red-shifted by 20 nm relative to that of the monosubstituted terthiophene (λ_{em} = 446 nm).[43]

Table 4. Emission Data for **1−8**, and **10−11** in Dichloromethane Solution

cpd	λ_{abs}/nm (ε/dm^3·mol^{-1}·cm^{-1})^a	λ_{em} /nm^b	OD^e	I^f	Q/Q_R^{g}
T_3	354 (28200)	410, 430^c 407, 426 ^{c}	0.110	1.00	1.00
1	383 ^{d}	465 ^{d}			
2	373 (20300)	430, 454	0.0809	1.96	2.67
3	377 (19300)	435, 462	0.0769	0.629	0.900
4	387 (35500)	475	0.141	0.857	0.669
5	374 ^{d}	446 ^{d}			
6	368 (20500)	450	0.0812	0.697	0.944
7	401 (37000)	477	0.143	1.50	1.15
8	377 (21300)	456	0.0845	1.16	1.51
10	387 (12800)	439, 462	0.0510	0.606	1.31
11	411 (47800)	475	0.190	0.565	0.327

[a] Linear absorption band maximum in CH_2Cl_2 solution. [b] Emission band maximum in CH_2Cl_2 solution. [c] First (upper) values were measured for CH_2Cl_2 solutions. Second (lower) values are from reference 48 and are for dioxane solutions. [d] Data are from reference 43 and are for hexanes solutions. [e] Optical density or absorbance at the excitation wavelength. [f] Integrated fluorescence intensity from the corrected fluorescence spectrum. The values reported are the ratio based on T_3. [g] The ratio of the quantum yields using T_3 as the internal reference. See eq 3.

The solution phase emission spectra for compounds **2−4**, **6−8**, and **10−11** (summarized in Table 4) show maximum emission bands in the blue region (between 430 and 480 nm), and are red-shifted relative to that of terthiophene (T_3: λ_{em} = 410, 430 nm).[48] Figure 4a shows the representative excitation and emission spectra for compound **2** with two emission bands at 430 and 454 nm, respectively, similar to those seen in other oligothiophenes.[49] The corresponding excitation spectra for these two emission bands were identical to their absorption spectra, which indicates the presence of a single species in the ground state. Figure 4b shows the comparison of the intensity of the emission spectra for compounds **2**, **3**, **6**, and **8** under the condition that the optical densities of the solutions are identical at the excitation wavelengths. For better comparison, the relative quantum yields (Q/Q_R) for all the compounds were calculated

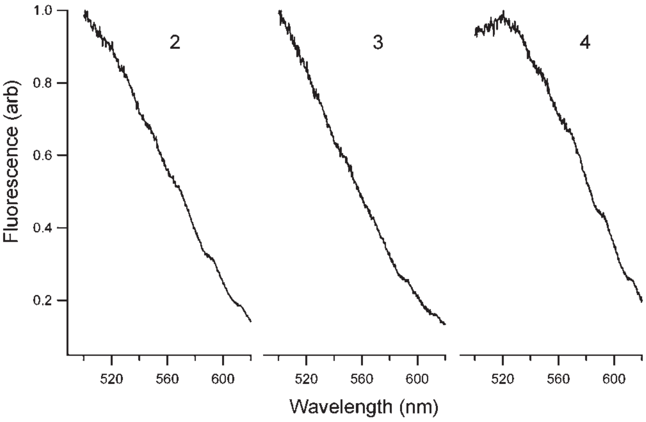

Figure 5. Thin film fluorescence emission spectra for **2**, **3**, and **4**, using the 457 nm Ar ion laser line for excitation.

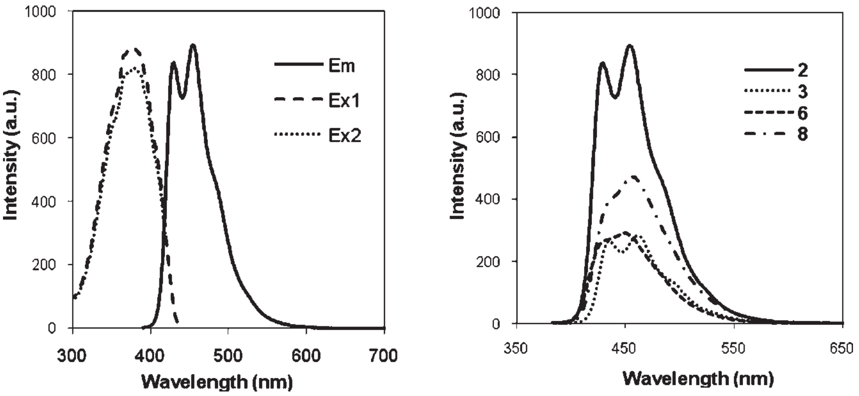

Figure 4. Left (a): excitation and emission spectra for **2**; excitation spectrum 1 (dashed line): λ_{Em} = 454 nm; excitation spectrum 2 (dotted line): λ_{Em} = 430 nm. Right (b): emission spectra of the 4 × 10^{-6} mol/L solutions of **2**, **3**, **6**, and **8** with identical optical density of 0.080 at their excitation wavelengths in a 10 mm cell.

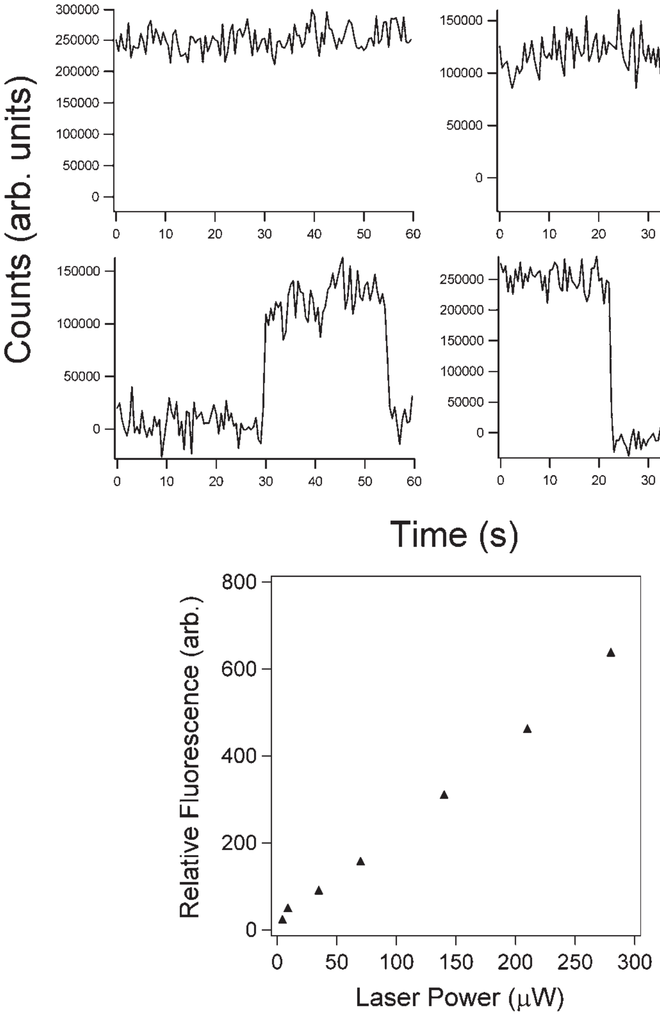

Figure 6. Single molecule fluorescence time traces for **4** showing stable emission (top), blinking (center left), and photobleaching (center right) and thin film fluorescence emission for **4** as a function of laser power for **4** using the 457 nm Ar+ laser line for excitation (bottom).

using the CH_2Cl_2 solution of T_3 as the reference solution (summarized in Table 4).

A comparison of the emission spectra for the mono- and disubstituted terthiophenes shows the effect of adding diphenyl(oxo)phosphino groups to the terthiophene (T_3: λ_{em} = 410, 430 nm; **6**: λ_{em} = 450 nm; **2**: λ_{em} = 430, 454 nm). Adding the first group (T_3 versus **6**) causes a significant red shift but no significant change is observed when the second group is added (**2** versus **6**) at the 5″-position of the terthiophene moiety. To our surprise, the introduction of the second diphenyl(oxo)phosphino group significantly affects the fluorescence quantum yield with **2** exhibiting much higher quantum yield than **6**.

A comparison of the emission spectra for the disubstituted terthiophenes **2**, **3**, and **4** shows the effect of the group on the phosphorus lone pair on the emission spectra. Although the substituent on the phosphorus does not significantly affect the emission maximum, it does affect the fluorescence quantum yield with **3** (S) and **4** (Me^+) having much lower quantum yields than does **2** (O).

A comparison of the emission spectra for the monosubstituted terthiophenes shows the effect of changing the functional *R*-group at the 5″-position. Compounds **7** (*R* = CHO), **8** (*R* = CH_2OH), and **10** (*R* = CO_2Me) show higher quantum yields than does **6** (*R* = H). However, compound **11** (*R* = CHNPh) shows relatively lower quantum yield than does **6**.

Thin Film and Single Molecule Fluorescence Spectra. Some of the most important applications for fluorescent materials involve emission from the solid state.[50,51] Thin film fluorescence spectra from the disubstituted terthiophenes **2**, **3**, and **4** were recorded so that the solid state emission characteristics could be compared to those of the compounds in solution. A comparison of the thin film emission spectra for disubstituted terthiophenes **2**, **3**, and **4** is shown in Figure 5. All three exhibit intense solid state and single molecule emission using 457 nm cw laser excitation with **4** exhibiting the longest wavelength emission of the three compounds. Emissions

---

(46) Woodward, R. B. *J. Am. Chem. Soc.* **1941**, *63*, 1123–1126.

(47) Valeur, B. *Molecular Fluorescence: Principles and Applications*; Wiley-VCH: Weinheim, Germany, 2002.

(48) Becker, R. S.; Seixas de Melo, J.; Macuanita, A. L.; Elisei, F. *J. Phys. Chem.* **1996**, *100*, 18683–18695.

(49) DiCésare, N.; Belletête, M.; Marrano, C.; Leclerc, M.; Durocher, G. *J. Phys. Chem. A* **1998**, *102*, 5142–5149.

(50) Noda, T.; Ogawa, H.; Noma, N.; Shirota, Y. *Appl. Phys. Lett.* **1997**, *70*, 699–701.

(51) Kim, D.; Salman, S.; Coropceanu, V.; Salomon, E.; Padmaperuma, A. B.; Sapochak, L. S.; Kahn, A.; Bredas, J.-L. *Chem. Mater.* **2010**, *22*, 247–254, and references therein.

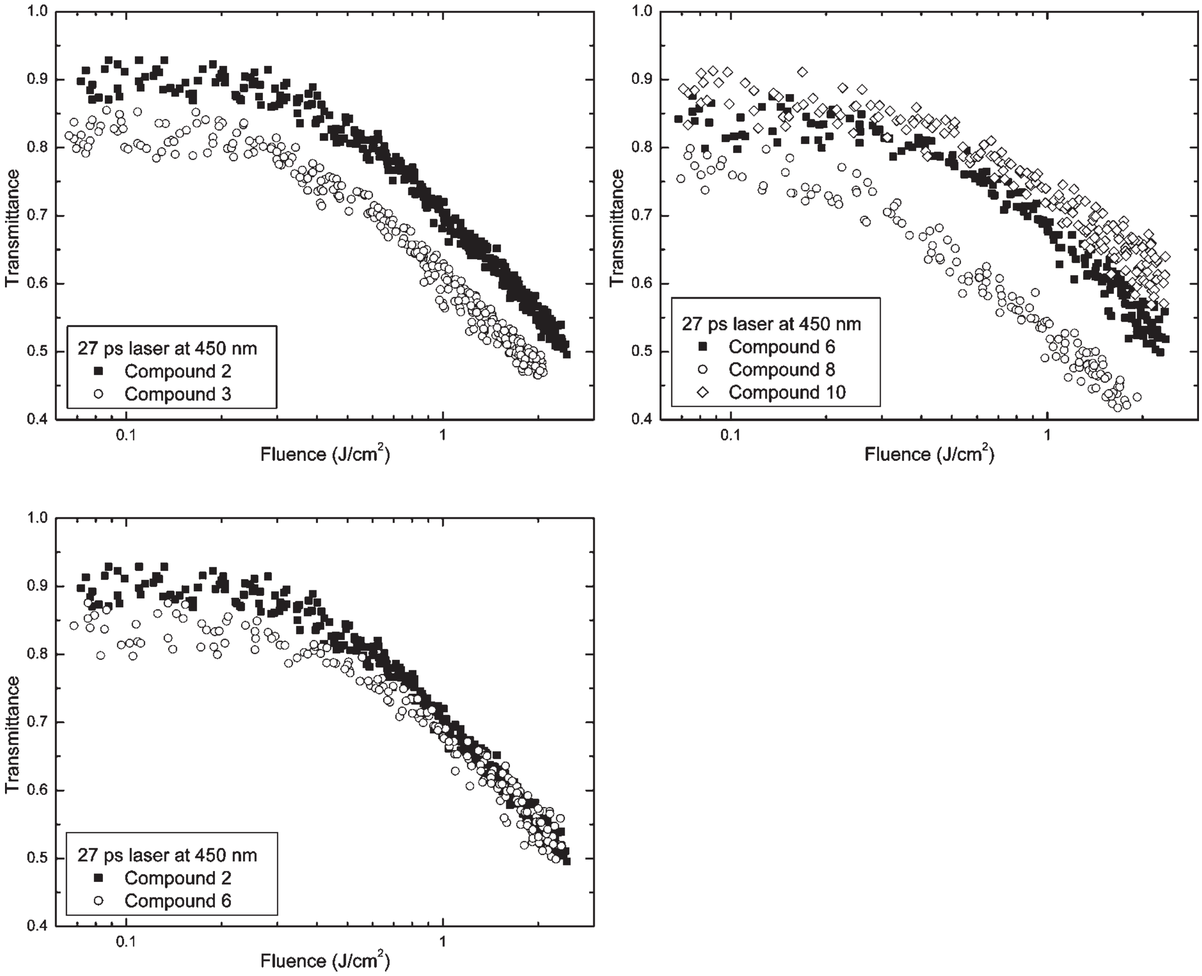

Figure 7. Comparison of the nonlinear transmittances of dichloromethane solutions of **2** and **3** (upper left), **2** and **6** (lower left) and **6**, **8**, and **10** (upper right) in a 1 mm cell as a function of incident energy with a 27 ps laser pulses at 450 nm.

from all three are truncated because of the dichroic and emission filters employed with the 457 nm laser excitation. The emission from **2** and **3** continually decreases above 500 nm and is consistent with the solution phase measurements. An emission maximum in **4**, however, is observed at 520 nm in the thin film spectrum, suggesting a red-shift in the solid state emission spectrum compared to solution measurements.

Thin film and single molecule fluorescence emissions from the disubstituted terthiophenes **2**, **3**, and **4** were obtained as function of laser power to investigate the possibility of NLA manifested in the fluorescence emission. Representative fluorescence time traces from single **4** molecules are shown in Figure 6a. The single disubstituted terthiophene molecules exhibit both blinking and photobleaching in the solid state,[52] and for this reason fluorescence measurements as a function of laser power were inconclusive. Thin film fluorescence requirements as a function of laser power for **4**, which exhibits the largest absorption and most intense emission of the three disubstituted terthiophenes with 457 nm excitation, are shown in Figure 6b. These results are representative of those of **2** and **3** in that thin film emission for all three compounds was observed to increase linearly with laser power. This suggests that higher peak laser power (such as that employed for the NLA results discussed below) is probably required to observe nonlinear effects in the fluorescence emission. This could not be done using cw excitation because laser powers above 300 μW result in rapid irreversible photobleaching of the thin films.

Nonlinear Optical Characterization. Because NLA is very dependent on wavelength, we have characterized the NLA of the compounds described in this manuscript over a range of wavelengths in the blue and green spectral regions near their linear absorption peaks. NLA measurements were performed on dichloromethane solutions of **2**–**8**, and **10**–**11** whose concentrations were between 3.50×10^{-3} and 3.65×10^{-3} mol/L in a 1 mm cuvette. To observe non-resonant NLA, linear transmittance must be large (greater than 70% for our system). On the basis of the linear absorption data discussed previously, **2**, **3**, **6**, **8**, and **10** have linear transmissions above 70% at 450 nm, all compounds except **11** have linear transmissions above 70% at 480 nm and all compounds have linear transmissions above 90% at 532 nm. Figures 7, 8 and 9 show the nonlinear transmittance of compounds at 450 nm, 480 and 532 nm, respectively.

At 450 and 480 nm, all compounds with linear transmittances > 70% exhibit significant NLA as the input energy is increased. The threshold of the NLA, defined as the incident

---

[52] Odoi, M. Y.; Hammer, N. I.; Rathnayake, H. P.; Lahti, P. M.; Barnes, M. D. *ChemPhysChem* **2007**, *8*, 1481–1486.

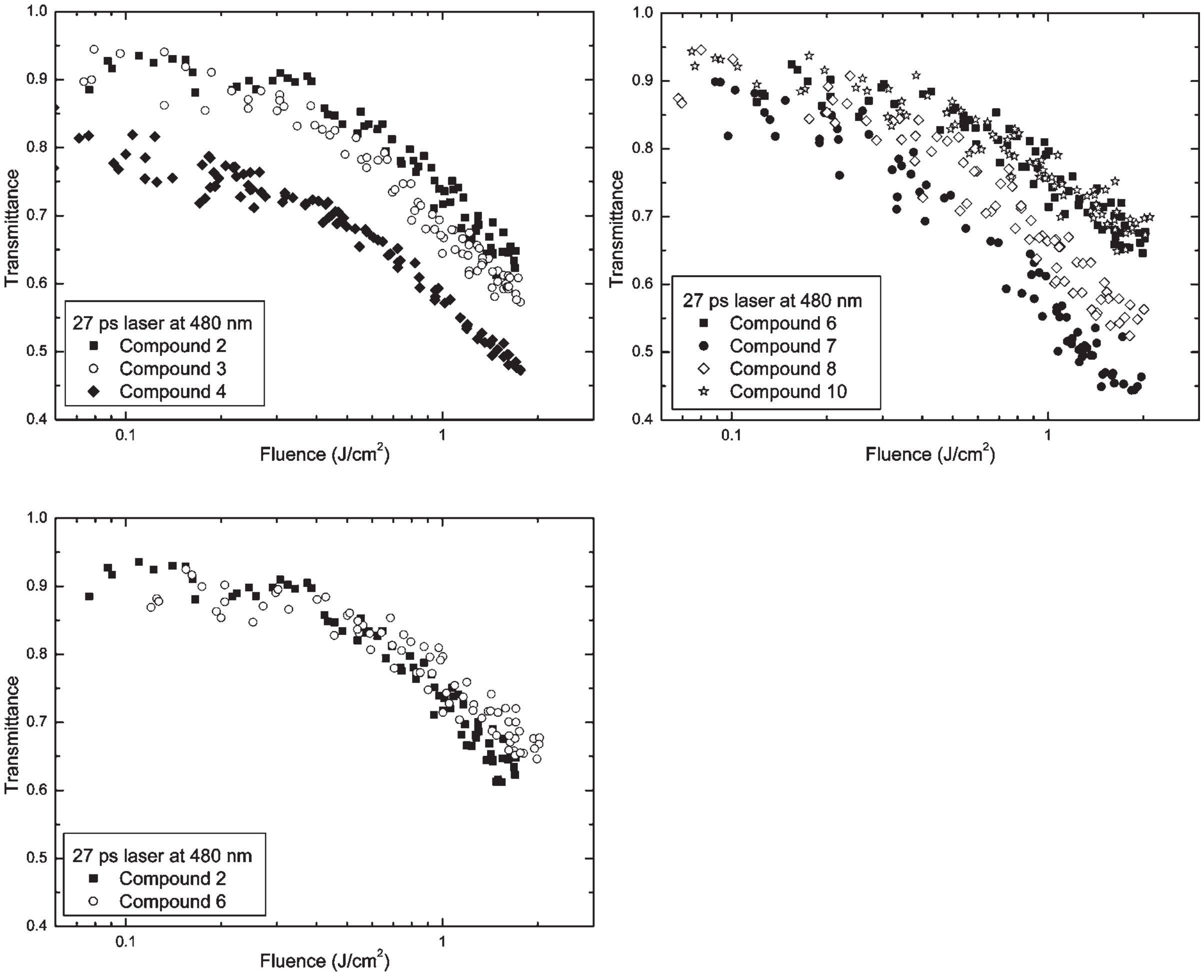

Figure 8. Comparison of the nonlinear transmittances of dichloromethane solutions of **2**, **3**, and **4** (upper left), **2** and **6** (lower left) and **6**, **7**, **8**, and **10** (upper right) in a 1 mm cell as a function of incident energy with 27 ps laser pulses at 480 nm.

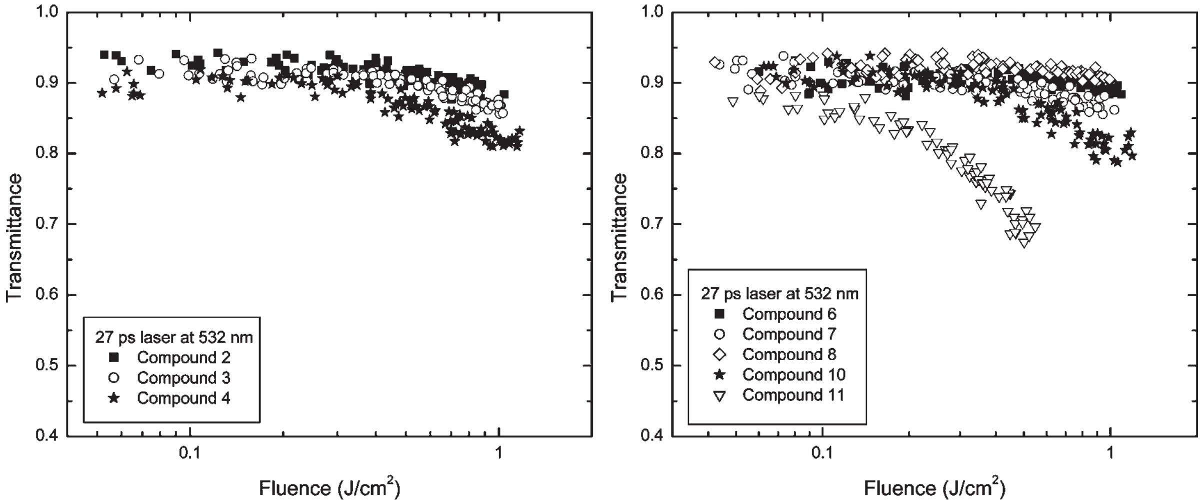

Figure 9. Comparison of the nonlinear transmittances of dichloromethane solutions of **2**, **3**, and **4** (left) and **6**, **7**, **8**, **10**, and **11** (right) a 1-mm cell as a function of incident energy with 27 ps laser pulses at 532 nm.

fluence at which the transmittance starts to deviate from the linear transmittance, is about 0.3 J/cm^2. At 450 nm, all of the NLA curves have approximately the same shape, and the major factor determining the NLA appears to be the linear absorption. Slight changes in the curve shape because of the terthiophene substituents are observed as shown by the plot of the NLA curves of **2** and **6**. It is interesting that the addition of a second diphenyl(oxo)phosphine group to the terthiophene shifts the linear absorption maximum closer to 450 nm but slightly weakens the NLA at that wavelength.

The NLA at 480 nm is somewhat weaker than is the NLA at 450 nm for all the compounds (transmittance at

1.7 J/cm^2: **2**, 59% versus 63%; **3**, 50% versus 59%, **6**, 58% versus 68%; **8**, 44% versus 55%; **10**, 66% versus 69%). In the case of **3**, this decrease appears to be primarily due to the decrease in linear absorption, but in the cases of **6**, **8**, and **10**, which have approximately the same linear absorption at 480 nm, the NLA curve of **8** is significantly steeper than are those of **6** and **10**. The NLA curve for **7**, whose NLA could not be measured at 450 nm because of its low linear transmittance at that wavelength, is even steeper (transmittance at 1.7 J/cm2: 50%) than is that of **8** demonstrating that the 2″-substitutent can have a significant effect on the NLA at a given wavelength.

At 532 nm, **11** exhibits the strongest NLA although its linear transmittance is 88% at this wavelength. Perhaps this is because 532 nm is considerably closer to the linear absorption peak of **11** than to those of any of the other compounds. It is also interesting that **10** still exhibits some NLA absorption at 532 nm. This makes it the broadest band nonlinear absorber of all of the terthiophene derivatives in this paper.

Conclusions

Terthiophenes with at least one diphenylphosphino-derived substituent exhibit NLA in the blue spectra region. For each of the terthiophene derivatives, the NLA is strongest at wavelengths near the linear absorption maximum of the compound. In addition, the group at the 5″-position of the terthiophene has a significant effect on the NLA as well as on both the linear absorption maximum and the emission maximum of the compound. This means that the strength of the NLA and the wavelength at which the NLA is observed can be varied by the appropriate choice of the 5″-substituent and the group attached to the nonbonding pair of electrons on the diphenylphosphino substituent. The introduction of functional groups at the 5″-position of the terthiophene also means that it should be possible to attach these nonlinear absorbers to polymers for use in oriented thin films or nanoparticles to generate hybrid nonlinear absorbing materials.

The emission spectra for all of these terthiophene derivatives show maximum emission bands in the blue region. Both the emission maxima and fluorescence quantum yields can be tuned by varying the 5″-substituent, the group attached to the phosphorus atoms, and the number of the phosphorus-donor groups with compound **2** exhibiting the strongest fluorescence emission intensity. These results suggest that materials with even higher quantum efficiencies could be prepared by increasing the number of thiophene units. Thin film fluorescence measurements also indicate that these materials might serve as good blue emitters in the solid state.

Acknowledgment. The authors gratefully acknowledge an Army Research Laboratories Cooperative Agreement (W011NF-06-2-0033) and NSF Cooperative Agreements (EPS-0814103 and EPS-0903787) for support of this research.

Supporting Information Available: Crystal structure data for **2** including tables of atomic coordinates, anisotropic thermal parameters, all bond lengths and angles, and hydrogen isotropic displacement parameters using the crystallographic information file (CIF) format. This material is available free of charge via the Internet at http://pubs.acs.org.